行政院國家科學委員會專題研究計畫 期末報告

鎳基超合金熱變形行為分析及組合關係探討

計 畫 類 別 ：個別型
計 畫 編 號 ：NSC 101-2221-E-216-007-
執 行 期 間 ：101 年 08 月 01 日至 102 年 07 月 31 日
執 行 單 位 ：中華大學機械工程學系

計 畫 主 持 人：吳泓瑜

計畫參與人員：碩士班研究生-兼任助理人員：朱峰君
碩士班研究生-兼任助理人員：吳政道

報 告 附 件 ：出席國際會議研究心得報告及發表論文

公 開 資 訊 ：本計畫可公開查詢

中 華 民 國 102 年 10 月 03 日

中 文 摘 要 ： 本研究主要探討鎳基超合金 Hastelloy X 在高溫下的熱變形機制及組合關係。使用熱壓縮實驗數據進行分析，其變形條件為溫度 950~1150 ˚C，應變速率 0.001~1 s-1。流變應力、溫度、應變速率的組合關係，以峰值應力為基礎來獲得組合方程式中的主要參數。同時也以變形後試件之金相微結構觀察，來分析熱變形條件對微結構變化的影響。由流變行為及微結構分析得知，鎳基超合金 Hastelloy X 在低溫主要的軟化機制為動態回復(Dynamic recovery)，高溫的軟化機制為動態再結晶(Dynamic recrystalliztion)或是動態再結晶加上晶粒成長。組合關係分析顯示，鎳基超合金 Hastelloy X 並不需要由指數及冪次律來決定應力指數 α。由指數及冪次律關係所獲得之組合關係式，在計算流變應力時會有較大的誤差。在僅由雙曲線正弦函數律所獲得之組合關係式，則可得到較精確的流變應力計算值。

中文關鍵詞： 鎳基超合金 Hastelloy X、流變形為、動態再結晶，動態回復、組合方程式

英 文 摘 要 ： The compressive deformation behavior and constitutive analysis of Hastelloy X superalloy were investigated in the temperature range of 950 to 1150 ˚C and strain rate range of 0.001 to 1 s− on Gleeble-3500 thermo-simulation machine. The obtained experimental stress-strain data were used to establish strain-dependent constitutive equations. The correlation between the strain-dependent constitutive parameters and flow behavior was analyzed. The results showed that dynamic recovery was the main softening effect during hot deformation at low temperatures, while dynamic recrystallization or dynamic recrystallization with grain growth were the predominant softening mechanisms on deforming at high temperatures. The constitutive analysis showed that it was not necessary to use power and exponential laws to determine the strain-dependent stress multiplier（α） used in the hyperbolic sine-type constitutive equation. A comparatively high scattering in the calculated stresses was found in the analysis with α determined by power and exponential laws, whereas better estimations between the experimental and calculated flow stresses were obtained in the analysis with α obtained according to hyperbolic

sine law.

英文關鍵詞： Ni-base superalloy Hastelloy X, Flow behavior, Dynamic recrystallization, Dynamic recovery, Constitutive equation

行政院國家科學委員會專題研究計畫成果報告

鎳基超合金熱變形行為分析及組合關係探討

Hot deformation behavior and constitutive analysis of Ni-base superalloy

計畫編號：NSC 101-2221-E-216-007

執行期間：101年 8月 1日至102年 7月31日

計畫主持人: 吳泓瑜　　中華大學機械工程學系教授

E-mail: ncuwu@chu.edu.tw

計畫參與人員：朱峰君、吳政道 中華大學機械工程學系研究生

中文摘要

本研究主要探討鎳基超合金Hastelloy X在高溫下的熱變形機制及組合關係。使用熱壓縮實驗數據進行分析，其變形條件為溫度950~1150 °C，應變速率0.001~1 s^{-1}。流變應力、溫度、應變速率的組合關係，以峰值應力為基礎來獲得組合方程式中的主要參數。同時也以變形後試件之金相微結構觀察，來分析熱變形條件對微結構變化的影響。由流變行為及微結構分析得知，鎳基超合金Hastelloy X在低溫主要的軟化機制為動態回復(Dynamic recovery)，高溫的軟化機制為動態再結晶(Dynamic recrystalliztion)或是動態再結晶加上晶粒成長。組合關係分析顯示，鎳基超合金Hastelloy X並不需要由指數及冪次律來決定應力指數α。由指數及冪次律關係所獲得之組合關係式，在計算流變應力時會有較大的誤差。在僅由雙曲線正弦函數律所獲得之組合關係式，則可得到較精確的流變應力計算值。

關鍵詞：鎳基超合金Hastelloy X、流變形為、動態再結晶，動態回復、組合方程式

Abstract

The compressive deformation behavior and constitutive analysis of Hastelloy X superalloy were investigated in the temperature range of 950 to 1150 °C and strain rate range of 0.001 to 1 s^{-1} on Gleeble-3500 thermo-simulation machine. The obtained experimental stress-strain data were used to establish strain-dependent constitutive equations. The correlation between the strain-dependent constitutive parameters and flow behavior was analyzed. The results showed that dynamic recovery was the main softening effect during hot deformation at low temperatures, while dynamic recrystallization or dynamic recrystallization with grain growth were the predominant softening mechanisms on deforming at high temperatures. The constitutive analysis showed that it was not necessary to use power and exponential laws to determine the strain-dependent stress multiplier (α) used in the hyperbolic sine-type constitutive equation. A comparatively high scattering in the calculated stresses was found in the analysis with α determined by power and exponential laws, whereas better estimations between the experimental and calculated flow stresses were obtained in the analysis with α obtained according to hyperbolic sine law.

Keywords: Ni-base superalloy Hastelloy X, Flow behavior, Dynamic recrystallization, Dynamic recovery, Constitutive equation

1. Introduction

The high temperature mechanical properties of the superalloys are strongly dependent on the changes in the microstructures during hot working [1,2]. Superalloys undergo work hardening, dynamic recovery (DRV) [3] and dynamic recrystallization (DRX) [4,5], leading to variations in the flow behavior during hot deformation. Changes in the microstructure because of theses metallurgical phenomena influences the deformation mechanism [6,7], which is dependent on deformation conditions, particularly temperature and strain rate. Understanding the hot deformation behavior of Hastelloy X superalloy is essential in optimizing its hot workability.

The effects of deformation temperature and strain rate on the hot deformation behavior are generally expressed by constitutive equations, which are often used to represent the flow behaviors of metals and alloys. McQueen and Ryan [8] indicated that the constitutive equation for creep is the power law, which is limited at a low stress. The exponential law is suitable for hot-working processes, but fails at high temperatures below a strain rate of 1 s^{-1}. Sellars and Tegart [9,10] introduced a hyperbolic sine constitutive equation that considers both power and exponential laws. The hyperbolic sine law combines the power law and the exponential law at low and high stress limits, respectively, thereby forming an expression that is suitable for analysis in hot-working processes.

The constitutive behavior in various metals and alloys has been investigated using different analytical, phenomenological and empirical models [11–23]. For instance, Phaniraj et al. [11] proposed a new relationship between the stress multipliers of hyperbolic constitutive equation in hot deformed modified 9Cr–1Mo (P91) steel. Mandal et al. [12] developed strain-dependent constitutive equations to predict high temperature flow stress in a Ti-modified austenitic stainless steel. Cai et al. [15] showed that the constitutive parameters can be expressed as polynomial functions of strain in a Ti–6Al–4V alloy. Krishnan et al. [16] predicted high temperature flow stress in 9Cr–1Mo ferritic steel during hot compression by use of constitutive equation incorporating compensation for both strain and strain rate. Constitutive modeling of 1Cr12Ni3Mo2VNbN martensitic steel based on the Arrhenius-type equation has been introduced by Xiao and Guo [18]. Maheshwari [20] established a new phenomenological material flow model to describe the dynamic deformation behavior of Al-2024 alloy.

The constitutive behavior of an annealed Hastelloy X supperalloy was investigated in this study. Hot compression tests were performed at various temperatures and strain rates. Based on the measured flow stress, the constitutive equations as a function of strain were established using strain-dependent constitutive parameters. In the analysis, two different methods were applied to determine the strain-dependent α used in the hyperbolic sine-type equations. In the first method, which has been adopted by most researchers, the strain-dependent α was estimated according to power and exponential laws. In the second method, only the hyperbolic sine law was considered to determine α. The obtained constitutive equations as a function of strain were validated by comparing the calculated flow stresses with experimental ones.

2. Materials and experimental procedure

The analyzed chemical composition (in wt%) of the annealed Hastelloy X superalloy rod used in this study was 22.1Cr, 17.8Fe, 9.2Mo, 1.48Co, 0.62W, and Ni balance. The initial microstructure of the as-received material is demonstrated in Fig. 1. Cylindrical specimens with a height of 9 mm and a diameter of 6 mm were machined out of the as-received stock along the axial direction for compression tests. Isothermal hot compression tests were conducted on the Gleeble 3500 thermal simulation machine at temperatures ranging from 950 to 1150 °C and at constant strain rates between 0.001 and 1 s^{-1}. The stimulator was equipped with a control system to induce the exponential decay of the actuator speed to achieve a constant strain rate. The specimens were lubricated with graphite foil to reduce friction at the punch-specimen interface. The specimen temperature was measured by means of a thermocouple spot-welded at the central region on the specimen surface. Before the samples were subjected to hot compression, the specimens were heated until the deformation temperature was reached. This deformation temperature was then kept constant for 3 min to eliminate thermal gradients and ensure the uniform temperature of the specimens. The decrease in height at the end of the compression tests was 50%, which corresponds to a true strain of approximately 0.7. The true stress-true strain curves were constructed using the load-stroke data obtained from the compression tests. The specimens were quenched with water immediately after they were subjected to hot compression.

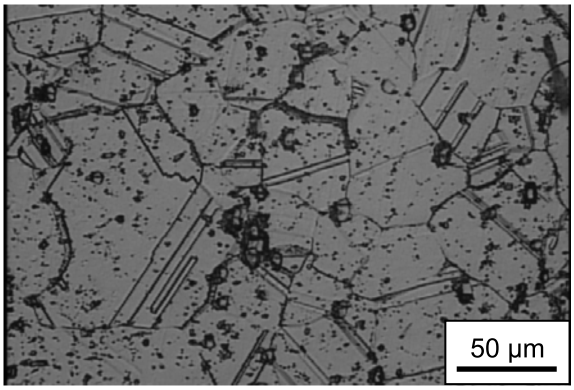

Fig. 1. Microstructure of the annealed Hastelloy X superalloy.

3. Results and discussion

3.1 Stress-strain curve and microstructure

Fig. 2 demonstrates the flow curves obtained at a strain rate of 1 s^{-1} and at a temperature of 950 °C. The flow curves exhibit typical flow behavior with dynamic softening. The flow stress increases due to work hardening at the onset of plastic deformation. The flow stress increases at a decreasing rate with increasing strain and

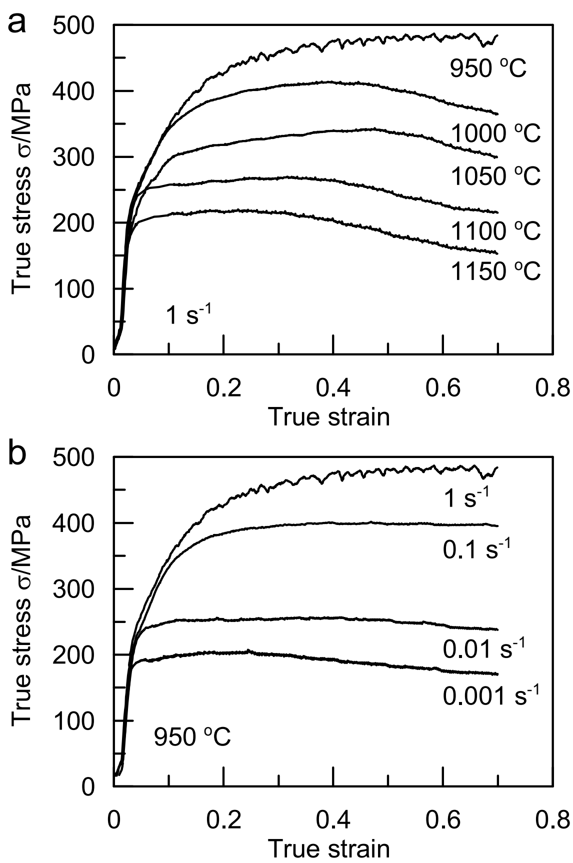

Fig. 2. Flow curves of the annealed Hastelloy X superalloy deformed at various temperatures and strain rates: (a) at 1 s^{-1} and (b) at 950 °C.

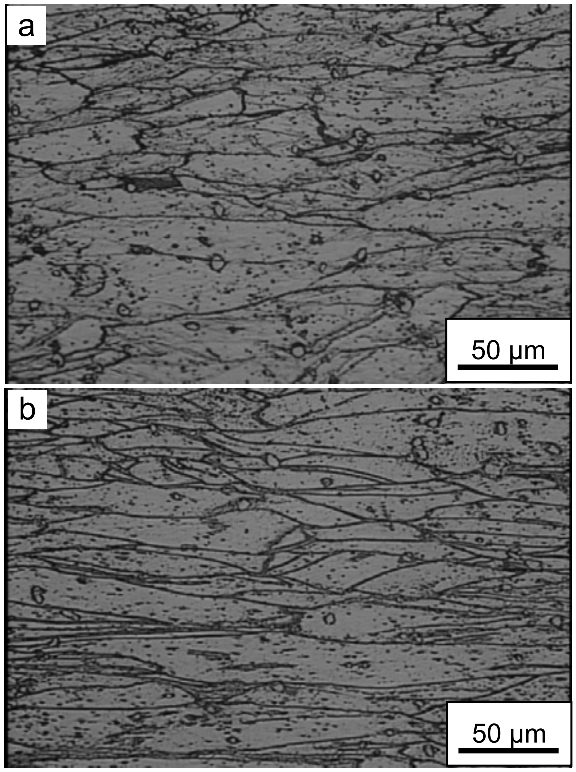

Fig.3. Microstructures of the specimens deformed at 950 °C and at two different strain rates: (a) at 1 s^{-1} and (b) at 0.001 s^{-1}.

reaches a peak value, after which the flow stress either decreases with increasing strain or reaches a steady-state value. The effects of the temperature and strain rate on the flow stress are significant for all test conditions. The flow stress level decreases with increasing temperature and decreasing strain rate. Fig. 3 shows the microstructures of the specimens deformed at 950 °C and at two different strain rates. Microstructures with elongated grains observed on deforming at the temperature of 950 °C suggest that DRV is the major softening effect under the deformation conditions of low temperatures [24]. Microstructures of the specimens deformed at 1150 °C and at two different strain rates are given in Fig. 4. Fine dynamically recrystallized grains found in the microstructure of the specimen deformed at 1150 °C and strain rate of 1 s^{-1} (Fig. 4a) indicates that DRX is the dominant softening mechanism. Microstructure with large grains observed on deforming at 1150 °C and strain rate of 0.01 s^{-1} (Fig. 4b) shows that DRX and grain growth are the main softening mechanisms.

3.2. Constitutive analysis with stress multiplier α determined by power and exponential laws

The constitutive equations of the power law, the exponential law, and the hyperbolic sine law can be expressed as Eqs. (1), (2), and (3), respectively:

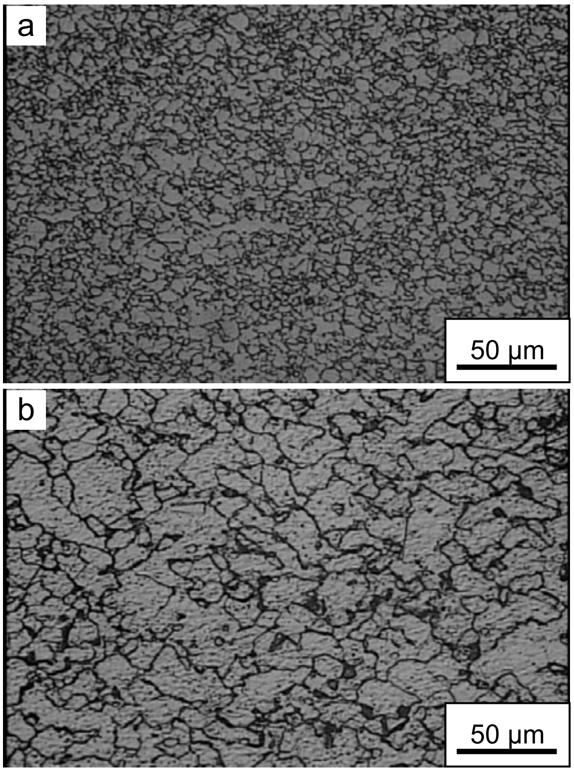

Fig. 4. Microstructures of the specimens deformed at 1150 °C and at two different strain rates: (a) at 1 s^{-1} and (b) at 0.01 s^{-1}.

$$\dot{\varepsilon} = A_1(\sigma)^{n_1} \exp\left[\frac{-Q}{RT}\right], \quad (1)$$

$$\dot{\varepsilon} = A_2 \exp(\beta\sigma)\exp\left[\frac{-Q}{RT}\right], \quad (2)$$

and

$$\dot{\varepsilon} = A[\sinh(\alpha\sigma)]^n \exp\left[\frac{-Q}{RT}\right], \quad (3)$$

where $\dot{\varepsilon}$ is the strain rate, α is the stress multiplier, n is the stress exponent, Q is the activation energy, R is the universal gas constant, and σ is the flow stress. A_1, A_2, A, n_1, and β are the material constants ($\alpha = \beta/n_1$). Taking the logarithm of both sides of Eqs. (1), (2), and (3) yield the following equations, respectively:

$$\ln\sigma = \frac{1}{n_1}\ln\dot{\varepsilon} - \frac{1}{n_1}\ln A_1 + \frac{Q}{n_1 R}\left(\frac{1}{T}\right), \quad (4)$$

$$\sigma = \frac{1}{\beta}\ln\dot{\varepsilon} - \frac{1}{\beta}\ln A_2 + \frac{Q}{\beta R}\left(\frac{1}{T}\right), \quad (5)$$

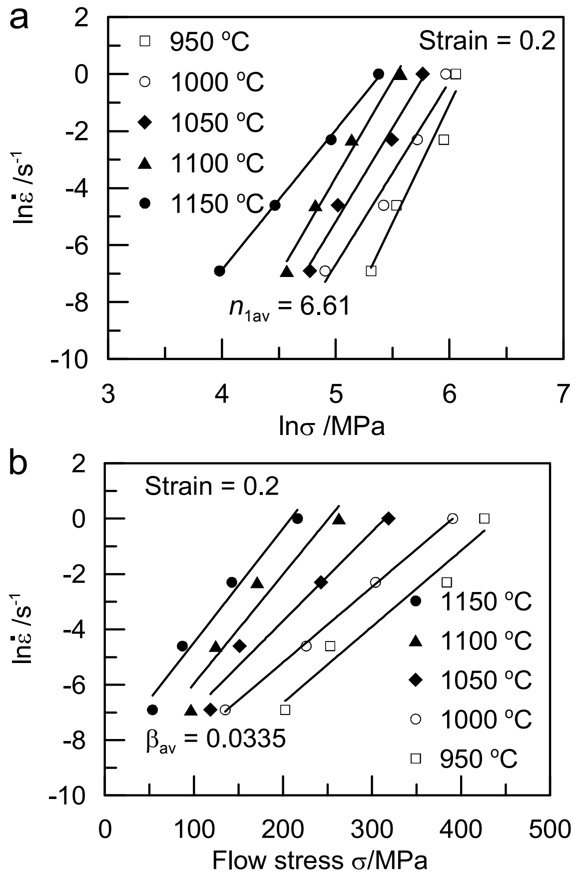

Fig. 5. Relationships between the strain rate and flow stress at a strain of 0.2: (a) $\ln\dot{\varepsilon}-\ln\sigma$ and (b) $\ln\dot{\varepsilon}-\sigma$.

and

$$\ln[\sinh(\alpha\sigma)] = \frac{1}{n}\ln\dot{\varepsilon} - \frac{1}{n}\ln A + \frac{Q}{nR}\left(\frac{1}{T}\right), \quad (6)$$

where n_1 and β are the slopes of the lines in $\ln\dot{\varepsilon}$–$\ln\sigma$ plot (Eq. (4)) and $\ln\dot{\varepsilon}$–σ plot (Eq. (5)) at a particular strain and temperature, respectively. Fig. 5 shows the relationships between the strain rate and the stress at a strain of 0.2. The calculated n_1 and β based on the slopes of the lines in Figs. 5a and 5b are 6.61 and 0.0335 MPa^{-1}, respectively. Thus, $\alpha = \beta/n_1 = 0.00507$ MPa^{-1}.

In Eq. (6), n is the slope of $\ln\dot{\varepsilon}-\ln[\sinh(\alpha\sigma)]$ plot at a particular strain and temperature. Q can be calculated using the slope of $\ln[\sinh(\alpha\sigma)]-1/T$ plot at a particular strain and strain rate. The relationships

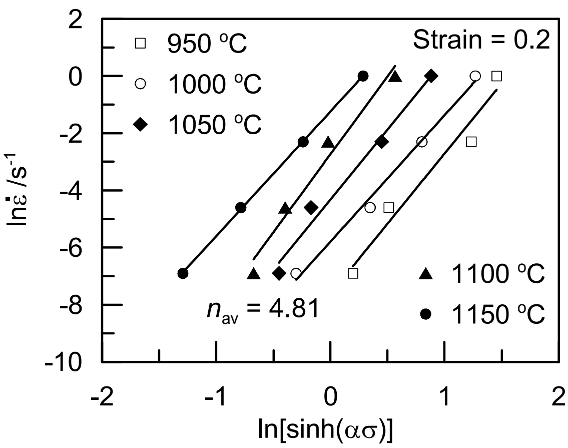

Fig. 6. Variation in $\ln\dot{\varepsilon}$ as a function of ln[sinh($\alpha\sigma$)] at various temperatures and a strain of 0.2.

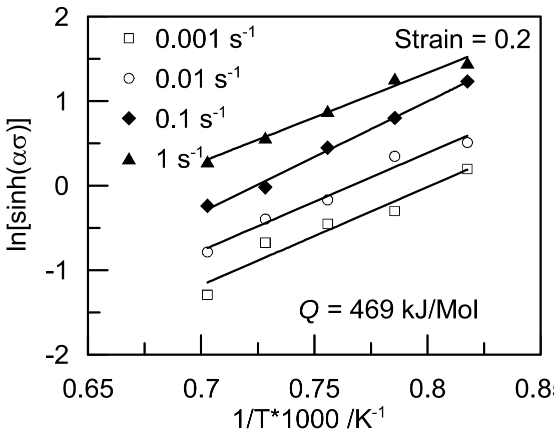

Fig. 7. Variation in ln[sinh($\alpha\sigma$)] as a function of reciprocal temperature at various strain rates and a strain of 0.2.

between the logarithmic strain rate ($\ln\dot{\varepsilon}$) and the logarithmic stress (ln[sinh($\alpha\sigma$)]) at a strain of 0.2 are given in Fig. 6. The value of the stress multiplier α used to calculate ln[sinh($\alpha\sigma$)] was equal to 0.00507 MPa^{-1}; which was obtained by power and exponential laws. The average value of stress exponent n estimated from Fig. 6 is 4.81. Fig. 7 illustrates the changes in flow stress as a function of reciprocal temperature. Q, which was calculated using the slopes of the plots in Figs. 6 and 7, is approximately 469 kJ/mol.

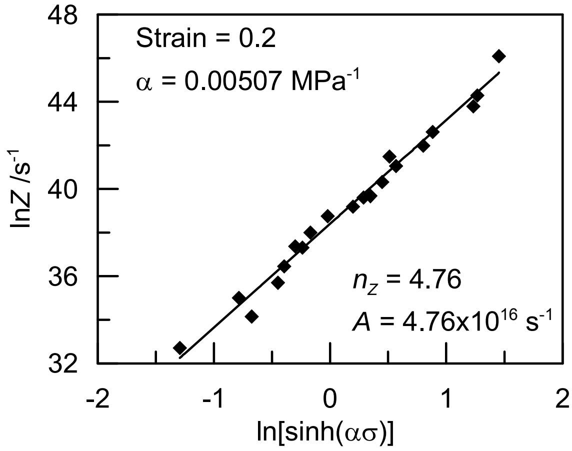

Fig. 8. Variation in ln$Z$ as a function of ln[sinh($\alpha\sigma$)] at various temperatures and a strain of 0.2.

Zener and Hollomon [25] showed that the effects of strain rate and temperature on hot deformation can be expressed by a compensated strain rate (Zener-Hollomon) parameter, Z, as shown below:

$$Z = \dot{\varepsilon}\exp\left[\frac{Q}{RT}\right] = A[\sinh(\alpha\sigma)]^n . \qquad (7)$$

Taking the natural logarithms of both sides of Eq. (7) yields the following equation:

$$\ln Z = \ln A + n\ln[\sinh(\alpha\sigma)] . \qquad (8)$$

A and n at a particular strain can then be obtained by plotting the relationship between lnZ and ln[sinh($\alpha\sigma$)]. The values of ln$A$ and n are the intercept and slope of ln$Z$ versus ln[sinh($\alpha\sigma$)] plot, respectively. Fig. 8 shows the ln$Z$ versus ln[sinh($\alpha\sigma$)] plot, indicating a fairly good linear fit with a coefficient of fit determination R^2 of 0.984. Thus, A at a strain of 0.2 obtained from Fig. 8 was 4.76 × 10^{16} s^{-1}.

Fig. 9 shows α, n, Q, and A as a function of strain. Q is the rate controlling parameter for hot deformation. Suery and Baudelet [26] explored constitutive equations according to the structure during deformation and

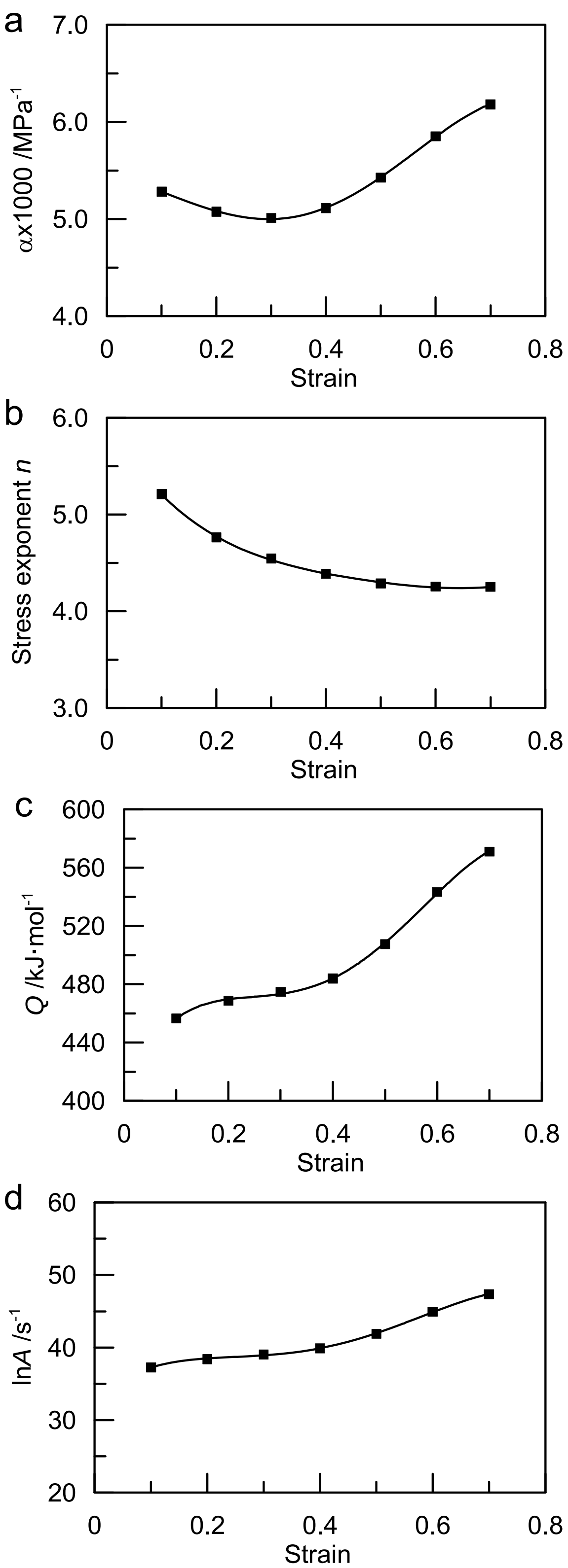

Fig. 9. Variations in the constitutive parameters as a function of strain with α determined by power and exponential laws: (a) α value; (b) n value; (c) Q value; and (d) ln$A$ value.

indicated that Q can vary with strain at a non-steady state flow condition; thus, Q is a non-unique parameter of the constitutive relationship for deformation at high temperatures. Variations in the constitutive parameters with strain can be related to the stress-strain behavior. At strains smaller than approximately 0.3, α and n decrease with increasing strain, whereas Q and A do not change significantly with increasing strain. This result satisfies the increase in flow stress with increasing strain at low strains in most flow curves (Fig. 2). The decreases in α and n with approximately constant Q and A meet the requirement for the increasing flow stress at low strains. At strains greater than approximately 0.3, increase in Q and decrease in n with increasing strain are balanced by increases in α and A with increasing strain to keep the decrease in flow stress as a response to dynamic softening at high strains.

Polynomial fittings are used to correlate the constitutive parameters with strain (Fig. 9). Hence, the strain-dependent constitutive equation with α determined by power and exponential laws for Hastelloy X superalloy can be expressed as follows:

$$\dot{\varepsilon} = A_\varepsilon[\sinh(\alpha_\varepsilon \sigma_\varepsilon)]^{n_\varepsilon} \exp\left[-\frac{Q_\varepsilon}{RT}\right], \qquad (9)$$

where $\alpha_\varepsilon = 0.0054 - 0.0002\varepsilon - 0.0159\varepsilon^2 + 0.0516\varepsilon^3 - 0.0373\varepsilon^4$,

$n_\varepsilon = 5.78 - 6.83\varepsilon + 10.45\varepsilon^2 - 5.48\varepsilon^3$,

$Q_\varepsilon = 405.6 + 810.5\varepsilon - 3716.7\varepsilon^2 + 7203.5\varepsilon^3 - 4379.2\varepsilon^4$, and

$\ln A_\varepsilon = 32.80 + 69.73\varepsilon - 311.15\varepsilon^2 + 597.03\varepsilon^3 - 360.55\varepsilon^4$.

The polynomial fittings for different constitutive parameters were chosen to

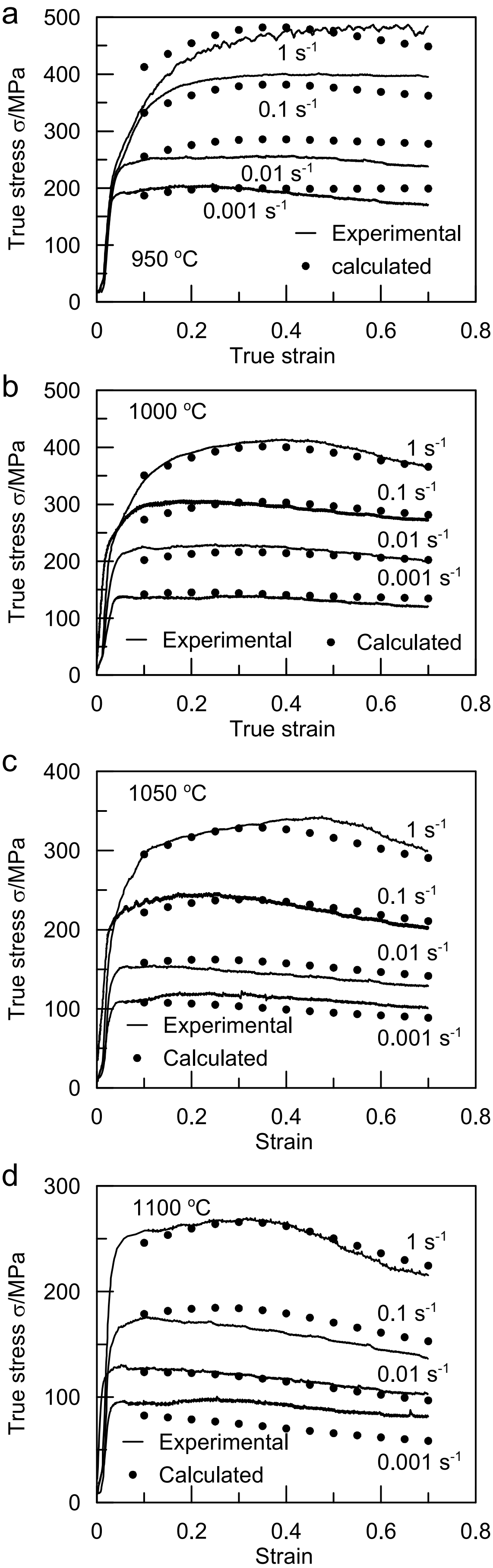

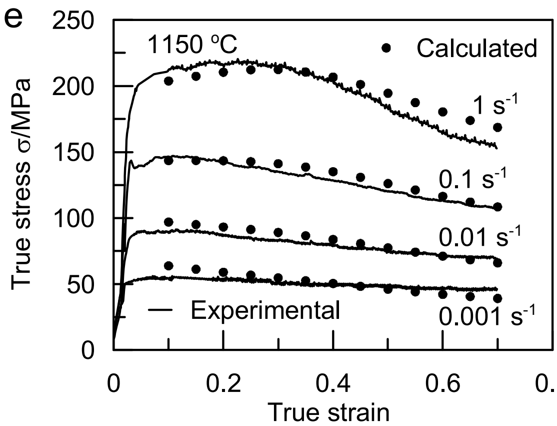

Fig. 10. Experimental and calculated flow stresses at various deformation conditions with α determined by power and exponential laws: (a) 950 °C; (b) 1000 °C; (c) 1050 °C; (c) 1100 °C; and (d) 1150 °C.

represent the influence of strain on the constitutive parameters with a good correlation.

Fig. 10 shows the comparisons of the experimental stress-strain curves and the stress values calculated using Eq. (9). The calculated flow stress is in reasonable agreement with the experimental flow curves, however, comparative large scattering could be observed at some deformation conditions. This scattering should result from the method which α was determined in the analysis. α is an adjustable constant that sets $\alpha\sigma$ into the correct range to make the lines in $\ln\dot{\varepsilon}-\ln[\sinh(\alpha\sigma)]$ plot parallel at a particular temperature. However, α cannot be adjusted in the hyperbolic sine constitutive equation in the analysis with α determined by power and exponential laws.

3.3. Constitutive analysis with α determined according to hyperbolic sine law

Eq. (6) shows that n is the slope of $\ln\dot{\varepsilon}-$

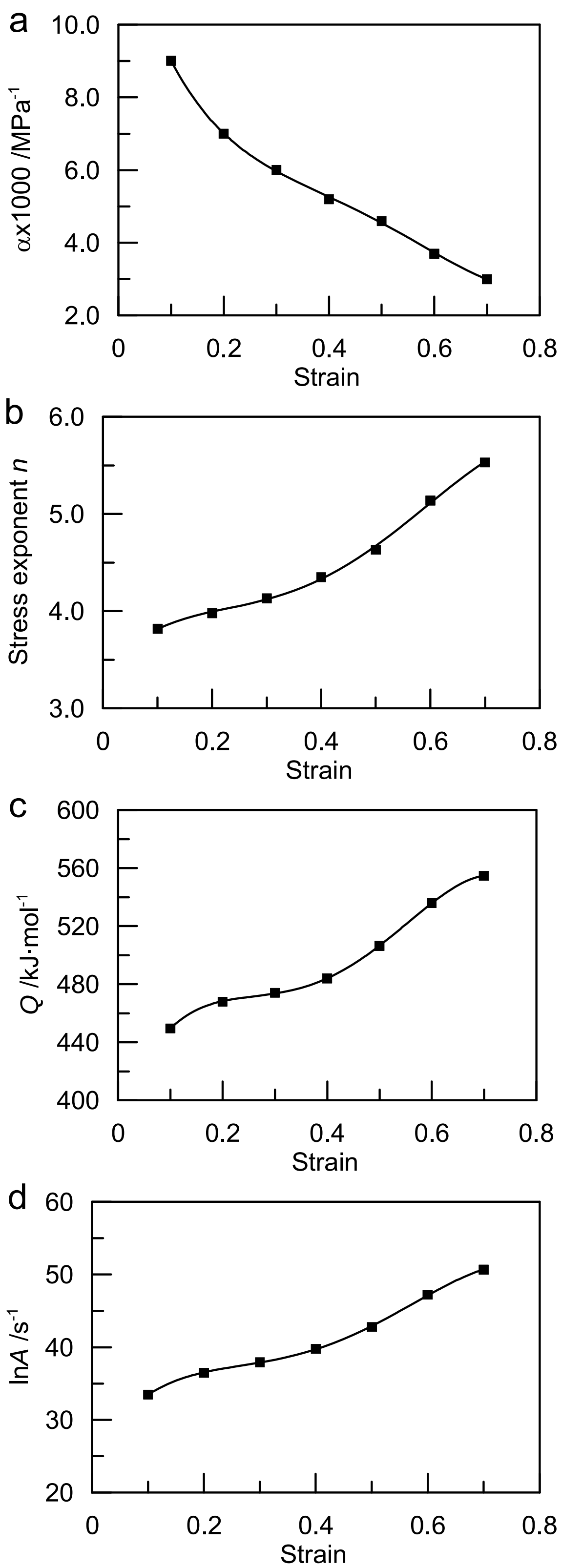

Fig. 11. Variations in the constitutive parameters as a function of strain with α determined by hyperbolic sine law: (a) α value; (b) n value; (c) Q value; and (d) ln$A$ value.

ln[sinh($\alpha\sigma$)] plot at a particular strain and temperature. α may be chosen based on the parallel lines that are obtained from the curves of $\ln \dot{\varepsilon}$ –ln[sinh($\alpha\sigma$)] plot without considering power and exponential laws. The parallelism of the $\ln \dot{\varepsilon}$ –ln[sinh($\alpha\sigma$)] lines can then be evaluated by the STDEV respect to the average n to determine α. α with a smaller STDEV with respect to the average n value shows a higher degree of parallelism. Detailed descriptions on the obtaining suitable α for hyperbolic sine-type constitutive analysis are given in the previous study [27].

Fig. 11 shows the values of α, n, Q, and A as a function of strain. α decreases with increasing strain, whereas n, Q, and A increase with increasing strain. At low strains, variations in n, Q, and A with strain are not so obvious, rapid decrease in α with increasing strain is the major factor to maintain the increasing flow stress (Fig. 2). At high strains, the decrease rate of α with strain decreases with increasing strain and approaches near constant rate, while the increases rates of n, Q, and A with strain increase with increasing strain. Decrease in α and increase in Q with increasing strain are balanced by increases in n and A with increasing strain to maintain the decline in the flow stress at high strains.

The effect of strain on the constitutive equation with α determined according hyperbolic sine law is also considered by using the constitutive parameters as a polynomial function of strain. Thus, the strain-dependent constitutive equation can be expressed as follows:

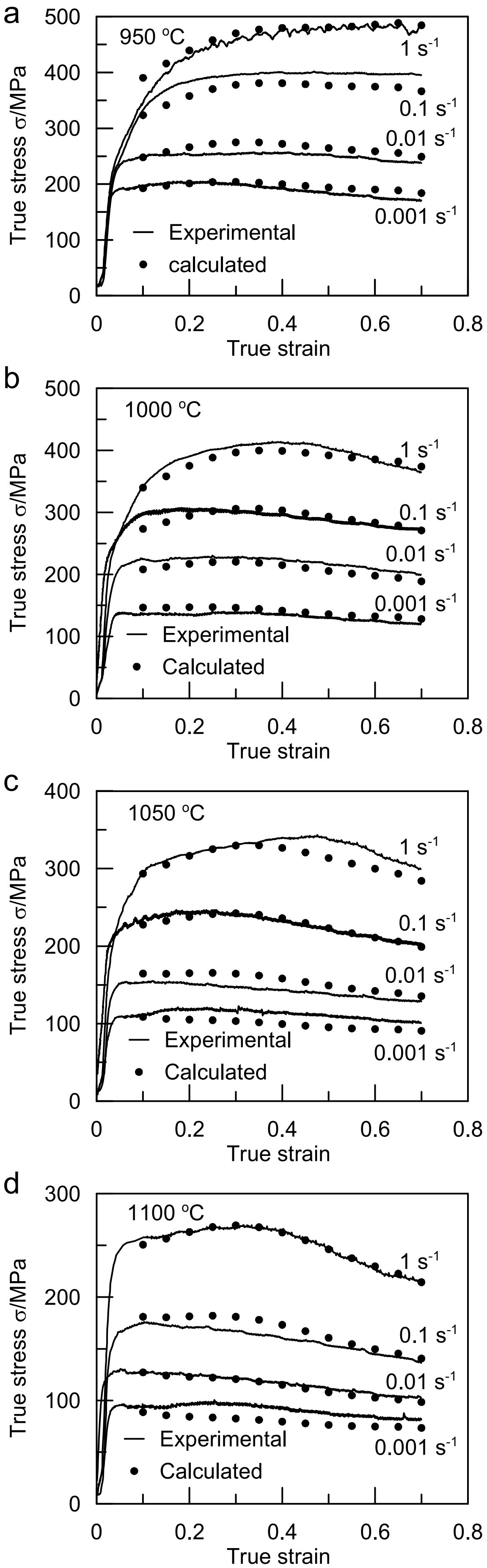

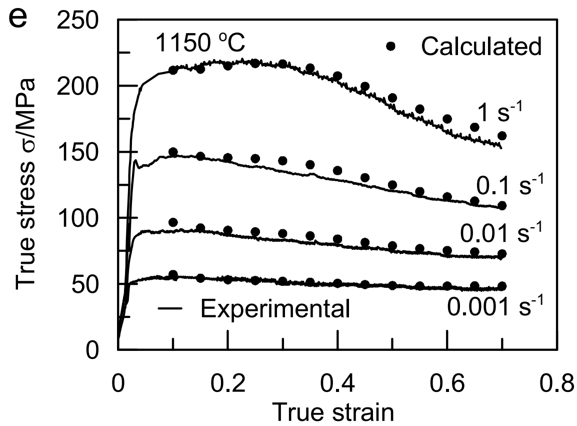

Fig. 12. Experimental and calculated flow stresses at various deformation conditions with α determined by hyperbolic sine law: (a) 950 °C; (b) 1000 °C; (c) 1050 °C; (c) 1100 °C; and (d) 1150 °C.

$$\dot{\varepsilon} = A_{\varepsilon}[\sinh(0.024\sigma_{\varepsilon})]^{n_{\varepsilon}} \exp\left[-\frac{Q_{\varepsilon}}{RT}\right], \quad (10)$$

where $\boldsymbol{\alpha}_{\varepsilon} = 0.0128 - 0.0508\varepsilon + 0.1471\varepsilon^2 - 0.2119\varepsilon^3 + 0.1098\varepsilon^4$,

$n_{\varepsilon} = 3.36 + 6.85\varepsilon - 28.51\varepsilon^2 + 57.66\varepsilon^3 - 35.10\varepsilon^4$,

$Q_{\varepsilon} = 386.1 + 988.8\varepsilon - 4314.2\varepsilon^2 + 8135.0\varepsilon^3 - 4997.2\varepsilon^4$, and

$\ln A_{\varepsilon} = 25.15 + 123.94\varepsilon - 494.13\varepsilon^2 + 902.50\varepsilon^3 - 535.86\varepsilon^4$.

Comparisons between the experimental and the predicted flow stresses calculated using Eq. (10) are given in Fig. 12. The calculated flow stress values are in good agreement with the experimental flow curves.

Figs. 10 and 12 also show that more accurate stresses are predicted using analysis with α determined according to the hyperbolic sine law. These results suggest that α is not necessary to be determined by power and exponential laws. Determining α by the parallel $\ln\dot{\varepsilon}$–$\ln[\sinh(\alpha\sigma)]$ lines can accurately predict the stress-strain relationships and simplify the analysis procedure to obtain the strain-dependent constitutive parameters for constitutive equation construction in Hastelloy X superalloy.

4. Conclusions

In this study, hot compression tests were carried out to investigate the hot deformation behavior of an annealed Hastelloy X superalloy. A constitutive modeling of the flow stress was also performed. The constitutive parameters α, n, A and activation energy Q were calculated by compensation of strain using polynomials. Considering the strain-dependent α obtained according to power and exponential laws, higher deviations were obtained with respect to average n at low and high strains. Thus, a comparatively higher scattering was observed on the predicted flow stress. The constitutive analysis with α determined by the parallel $\ln\dot{\varepsilon}$–ln[sinh($\alpha\sigma$)] lines showed that α could be estimated according to the hyperbolic sine equation, in which the obtained constitutive equation could provide better prediction in flow stress under the deformation conditions performed in this study. Comparisons between the experimental and predicted results confirmed that the developed constitutive equations could be used to numerically simulate the hot deformation of Hastelloy X superalloy. Constitutive analysis with α estimated according to hyperbolic sine law provided more accurate prediction capability in flow stress calculation.

References

[1] S. Guo, D. Li, H. Pen, Q. Guo, J. Hu, J. Nuclear Mater. 410 (2011) 52–58.
[2] S.L. Semiatin, P.N. Fagin, M.G. Glavicic, D. Raabe, Scripta Mater. 50 (2004) 625–629.
[3] N.D. Ryan, H.J. McQueen, Czech. J. Phys. B 39 (1989) 458–465.
[4] M. Jafari, A. Najafizadeh, Mater. Sci. Eng. A 501 (2009) 16–25.
[5] H. Mirzadeh, A. Najafizadeh, Mater. Design 31 (2010) 1174–1179.
[6] M. Aghaie-Khafri, N. Golarzi, J. Mater. Sci. 43 (2008) 3717–3724.
[7] W.Z. Abuzaid, M.D. Sangid, J.D. Carroll, H. Sehitoglu, J. Lambros, J. Mech. Phys. Solids 60 (2012) 1201–1220.
[8] H.J. McQueen, N.D. Ryan, Mat. Sci. Eng. A 32 (2002) 43–63.
[9] C. Sellars, W.M. Tegart, Acta Metall. 14 (1966) 1136–1138.
[10] C. Sellars, W.M. Tegart, Int. Metall. Rev. 17 (1972) 1–23.
[11] C. Phaniraj, D. Samantaray, S. Mandal, A.K. Bhaduri, Mater. Sci. Eng. A 528 (2011) 6066–6071.
[12] S. Mandal, V. Rakesh, P.V. Sivaprasad, S. Venugopal, K.V. Kasiviswanathan, Mater. Sci. Eng. A 500 (2009) 114–121.
[13] H. Mirzadeh, A. Najafizadeh, Mater. Sci. Eng. A 527 (2010) 1160–1164.
[14] G.L. Ji, F.G Li, Q.H. Li, H.Q Li, Z. Li, Mater. Sci. Eng. A 528 (2011) 4774–4782.
[15] J. Cai, F.G. Li, T.Y. Liu, B. Chen, M. He, Mater. Design 32 (2011) 1144–1151.

[16] S.A. Krishnan, C. Phaniraj, C. Ravishankar, A.K. Bhaduri, P.V. Sivaprasad, Int. J. Pres. Ves. Pip. 88 (2011) 501–506.
[17] A. Momeni, S.M. Abbasi, H. Badri, Appl. Math. Model. 36 (2012) 5624–5632.
[18] Y.H. Xiao, C. Guo, Mater. Sci. Eng. A 528 (2011) 5081–5087.
[19] H.Y. Li, Y.H. Li, D.D. Wei, J.J. Liu, X.F. Wang, Mater. Sci. Eng. A 530 (2011) 367–372.
[20] A.K. Maheshwari, Comp. Mater. Sci. 69 (2013) 350–358.
[21] D. Samantaray, C. Phaniraj, S. Mandal, A.K. Bhaduri, Mater. Sci. Eng. A 528 (2011) 1071–1077.
[22] Y.C. Lin, Q.F. Li, Y.C. Xia, L.T. Li, Mater. Sci. Eng. A 534 (2012) 654–662.
[23] H.R. Rezaei Ashtiani, M.H. Parsa, H. Bisadi, Mater. Sci. Eng. A 545 (2012) 61–67.
[24] T.H. Courtney, Mechanical Behavior of Materials, Second ed., McGraw-Hill Book Company, New York, 2000.
[25] C. Zener, J.H. Hollomon, J. Appl. Phys. 15 (1944) 22–27.
[26] M. Suery, B. Baudelet, Rev. Phys. Appl. 13 (1978) 53–66.
[27] H.Y. Wu, F.J. Zhu, S.C. Wang, W.R. Wang, C.C. Wang, C.H. Chiu, J. Mater. Sci. 47 (2012) 3971–3981.

行政院國家科學委員會補助國內專家學者出席國際學術會議報告

101 年 11 月 28 日

附件三

<table>
<tr><td>報告人姓名</td><td>吳泓瑜</td><td>服務機構
及職稱</td><td>中華大學機械系教授</td></tr>
<tr><td>會議 時間
地點</td><td>1011124~1011125
國際學術研討會
中國廣州</td><td>本會核定
補助文號</td><td>計畫編號
NSC 101-2221-E-216 -007</td></tr>
<tr><td>會議
名稱</td><td colspan="3">（中文）2012 應用力學及製造系統國際學術研討會
（英文）2012 International Conference on Applied Mechanics and Manufacturing System (AMMS2012)</td></tr>
<tr><td>發表
論文
題目</td><td colspan="3">（中文）Ni 基超合金 Hastelloy X 熱壓組合關係分析
（英文）Constitutive Analysis of Ni-Base Superalloy Hastelloy X under Hot Compression</td></tr>
</table>

報告內容應包括下列各項：

一、參加會議經過

1. 此項國際學術研討會於中國大陸廣州市東山賓館舉行，為期二天。
2. 會議於早上 9:00 於東山賓館一號樓凱旋廳展開，開幕由 Professor Renjun Gou 擔任 Keynote speaker 發表專題演講。
3. Keynote speech 於 10:20 結束，休息 20 分鐘後，10:40 開始進行各組之口頭報告。口頭報告每人以 10 分鐘為原則。本人參與之論文發表口頭報告安排於 24 日上午 11:10 分，報告完畢，與會者回響熱烈，提出相關問題討論。
4. 二十四日晚於東山賓館一號樓二樓餐廳舉辦晚宴，提供與會專家學者之交流機會。

二、與會心得

AMMS2012 委員會的成員包括美國的 George Mason University，澳大利亞的 University of Technology Sydney，韓國的 Hoseo University，泰國的 Suranaree University of Technology 及中國大陸的 Beijing Normal University…等。此次研討會的會議主題包括 Engineering Science for Manufacturing 及 Research on Manufacturing Process and Engineering Management of Manufacturing Systems 等兩大領域，共發表學術論文 198 篇。本人所參加的為 Engineering Science for Manufacturing 項主題，此項主題所發表之論共計 76 篇，論文內容包括理論分析及實驗驗證，分別探討機械設計、材料力學、材料腐蝕、機械加工及製程檢測等研究，論文內容豐富。參加此項會議，可以充分了解現階段各學術研究單位在應用力學及製造系統的研究趨勢及對未來在工業上應用的方向。此項會議就本人而言，可謂獲益良多。會議中並與相關領域的國外學者進行交流，提高本校之知名度。所有發表之論文均收錄於 Applied Mechanics and Materials Vol. 252 (2013)期刊論文中。

三、考察參觀活動(無是項活動者省略)

無

四、建議

應鼓勵國內教師多參予國際性學術研討會。

表 Y04

五、攜回資料名稱及內容

1. Applied Mechanics and Materials Vol. 252 (2013)論文集紙本。
2. 2012 International Conference on Applied Mechanics and Manufacturing System (AMMS2012) Conference Program Guide.

六、其他

Applied Mechanics and Materials Vol. 252 (2013) pp 73-76
© (2013) Trans Tech Publications, Switzerland
doi:10.4028/www.scientific.net/AMM.252.73

Constitutive Analysis of Ni-Base Superalloy Hastelloy X under Hot Compression Based on Thermodynamics

Horngyu Wu[1,a], Hsucheng Liu[1,b], Fengjun Zhu[1,c] and Chuihung Chiu[2,d]

[1]Department of Mechanical Engineering, Chung Hua University, Hsinchu, Taiwan

[2]Material and Chemical Research Laboratories, Industrial Technology Research Institute, Chutung, Taiwan

[a]ncuwu@chu.edu.tw, [b]m10008005@chu.edu.tw, [c]b09627016@chu.edu.tw, [d]davy@itri.org.tw

Keywords: Hastelloy X superalloy, Flow behavior, Dynamic softening, Constitutive analysis.

Abstract. Hot deformation characteristics of Hastelloy X Ni-base superalloy were investigated at elevated temperatures. Hot compressive tests were carried out in the temperature and strain rate ranges from 900 to 1150 °C and 0.001 to 1 s^{-1}, respectively. The constitutive equation relating flow stress, temperature, and strain rate was obtained based on the peak stresses. The flow behavior showed that the softening mechanisms were related to the dynamic recovery (DRV) and dynamic recrystallization (DRX). The flow stress of Hastelloy X was fitted well by the constitutive equation of the hyperbolic sine function. The constitutive analysis suggested that the hot deformation mechanism of the Hastelloy X was dislocation creep.

Introduction

The Hastelloy X Ni-base superalloy is solid-solution-strengthened with very good high-temperature strength and very good resistance to oxidizing environments up to about 1095°C. Applications include materials for fabricated or forged parts in gas turbine engines, and chemical and petrochemical plants, power plant and industrial heating applications. The high temperature mechanical properties of the superalloys are highly sensitive to flow characteristic and microstructural changes of the material during hot working [1,2]. An understanding of the flow behavior of the alloys is essential for optimizing workability and controlling microstructural evolution during hot working. During hot deformation, dynamic softening processes are operating simultaneously with deformation process. The hardening due to deformation process is relaxed by the softening process, such as dynamic recovery (DRV) and/or dynamic recrystallization (DRX) [3,4]. Deformation temperature and strain rate are the main parameters for controlling the microstructural softening effects. At temperatures above recrystallization temperature, the influence of strain rate becomes increasingly important and the degree of dependency of flow stress on temperature varies considerably among different materials.

In the present paper, the flow characteristics of Hastelloy-X superalloy are investigated by hot compression tests at various temperatures and strain rates. The study focuses on the effects deformation conditions on the flow characteristics during hot compression.

Experimental procedures

The experimental material was annealed Hastelloy X Ni-base superalloy rod with a chemical composition of Ni–22.1Cr–17.8Fe–9.2Mo–1.48Co–0.62W (wt%). Cylindrical specimens 6 mm in diameter and 9 mm high were machined out of the as-received stock for compression tests. The initial microstructure is demonstrated in Fig. 1. Hot compressed tests were conducted on a Gleeble-3500 thermal simulation machine at temperatures ranging from 900 to 1150 °C, at strain rates varying between 0.001 and 1 s^{-1}. Specimens were heated to the test temperature and kept for 3 min before hot compression. The initial height of the specimen was reduced to 50% corresponding to a true strain of approximately 0.7. The specimens were water quenched immediately after hot compression.

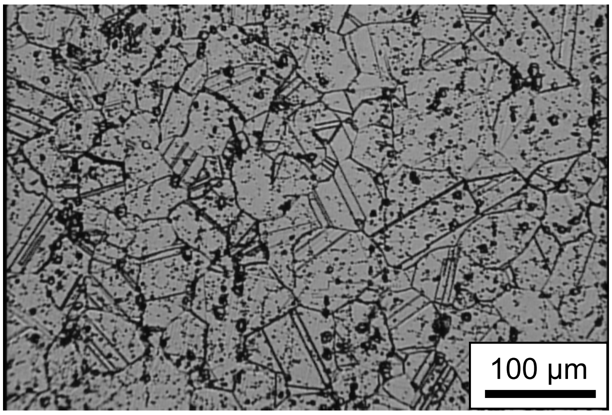

Fig. 1. Optical image of the initial microstructure of the Hastelloy X superalloy.

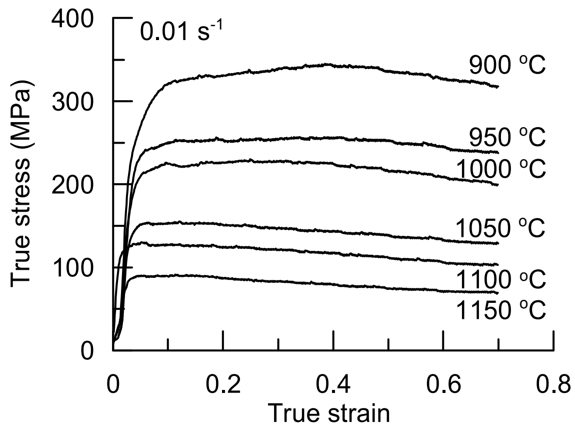

Fig. 2. Compression curves for the Hastelloy X at a strain rate of 0.01 s^{-1} and various temperatures.

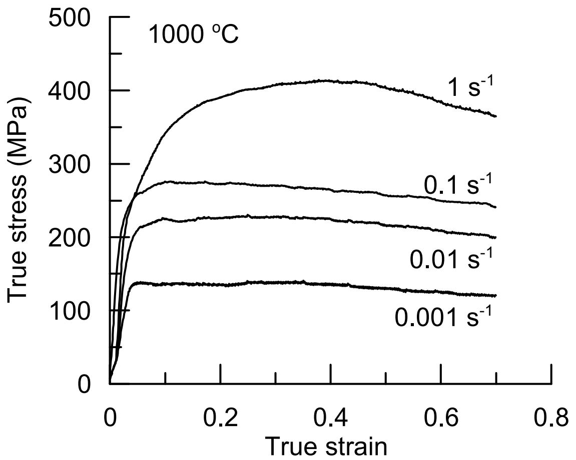

Fig. 3. Compression curves for the Hastelloy X at a temperature of 1000 °C and various strain rates.

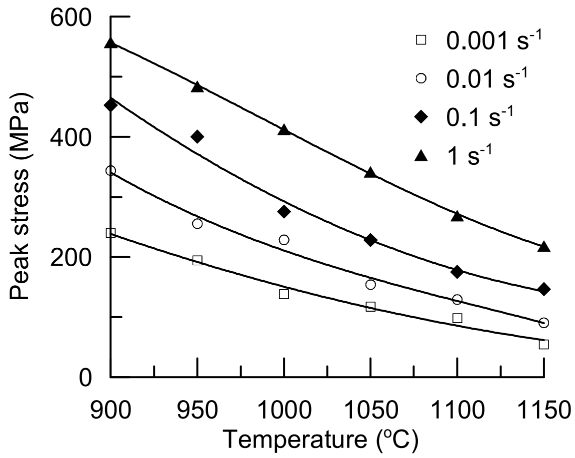

Fig. 4. Peak stress as a function of temperature at various strain rates.

Results and Discussion

Flow Behavior. Figs. 2 and 3 illustrate the stress–strain curves obtained at a strain rate of 0.01 s^{-1} and various temperatures (Fig. 2) and at a temperature of 1000 °C and various strain rates (Fig. 3). The flow curves exhibit the typical flow behavior with dynamic softening. The flow stress increases and reaches a peak value, after which the stress decreases with increasing strain, eventually reaching a steady-state value. At higher strain rates (or lower temperature), hardening followed by softening is more obvious, whereas at lower strain rates (or higher temperatures), a dynamic equilibrium between hardening and softening takes place at the very beginning of deformation. The initial rapid rise in stress is associated with an increase in dislocation density, as a result of strain hardening. At high strain rates, dislocation multiplication is more rapid than that at low strain rates and contributes to higher strain hardening effect. The flow curves with higher work hardening effect at higher strain rates (or lower temperatures) suggest that DRV may be the major softening effect, while DRX is the dominant softening mechanism at low strain rates (or higher temperatures).

Fig. 4 shows the variation in the peak stress as a function of temperature at various strain rates. The peak stresses are evidently dependent on the strain rate and temperature. The stresses increase with increasing strain rate at a fixed temperature. Moreover, they decrease with increasing temperature at a given strain rate. However, the extent of decrease depends on the temperature. The effect of the strain

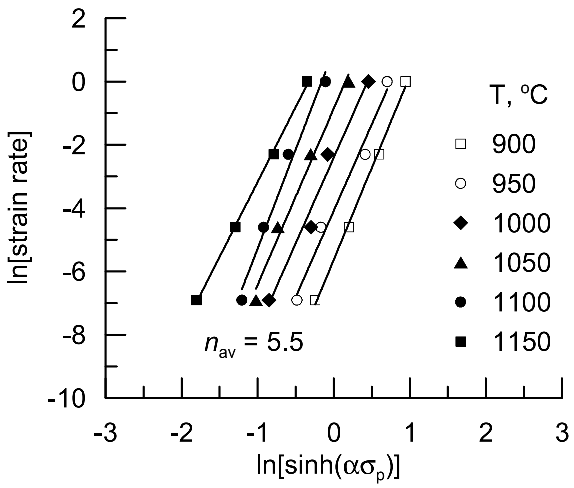

Fig. 5. Variation in $\ln\dot{\varepsilon}$ as a function of $\ln[\sinh(\alpha\sigma_p)]$ at various temperatures.

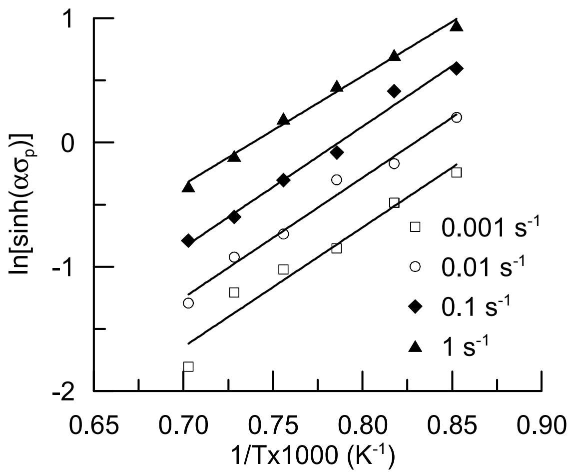

Fig. 6. Variation in $\ln[\sinh(\alpha\sigma_p)]$ as a function of reciprocal temperature.

rate on the stresses is more pronounced at low temperatures. The peak stress significantly decreases with increasing temperature at high strain rates. In contrast, the differences in the peak stress between different temperatures are smaller at low strain rates. Increasing strain rate at low temperatures leads to an increase in the dislocation density, resulting in higher-stress concentration regions. Therefore, peak stress increases noticeably with strain rate at low temperatures.

Constitutive analysis. The relation between the flow stress, deformation temperature, and strain rate is generally expressed by the hyperbolic sine law [5,6]

$$\dot{\varepsilon} = A[\sinh(\alpha\sigma)]^n \exp\left[\frac{-Q}{RT}\right], \tag{1}$$

where A (s^{-1}) and α (MPa^{-1}) are constants, σ is the flow stress (MPa), n is the stress exponent, and Q is the activation energy. The rate-controlling mechanism may be evaluated based on the activation energy. By taking the natural logarithms of both sides of Eq. (1), Equation (1) can be rewritten as

$$\ln[\sinh(\alpha\sigma)] = \frac{1}{n}\ln\dot{\varepsilon} + \frac{Q}{nR}\left(\frac{1}{T}\right) - \frac{1}{n}\ln A\,. \tag{2}$$

The value for α may be chosen in such a way that parallel lines could be obtained from the curve of $\ln\dot{\varepsilon}$ versus $\ln[\sinh(\alpha\sigma)]$. According to Eq. (2), n is the slope of the line in the plot of $\ln\dot{\varepsilon}$ versus $\ln[\sinh(\alpha\sigma)]$ at constant strain and temperature. The value of Q can be calculated using the slope of the line in the plot of $\ln[\sinh(\alpha\sigma)]$ versus $1/T$ at constant strain and strain rate.

The relationships between the logarithmic peak stress and the logarithmic strain rate ($\ln\dot{\varepsilon}$) are given in Fig. 5. The value of the stress multiplier α was equal to 0.003 MPa^{-1}; this yields the best fit of the experimental data. The average value of stress exponent n is 5.5. The n-value suggests that dislocation creep could be a dominant deformation process [7]. The variation in $\ln[\sinh(\alpha\sigma_p)]$ as a function of the reciprocal of the temperature is given in Fig. 6. The activation energy Q calculated using the slopes of the plots in Figs. 3 and 4 is 432 kJ/mol.

The constitutive equation could be related to the Zener−Hollomon parameter (Z), in which case Eq. (1) can be shown as [8]

$$Z \equiv \dot{\varepsilon}\exp[\frac{Q}{RT}] = A[\sinh(\alpha\sigma)]^n\,. \tag{3}$$

By taking the natural logarithms of both sides of Eq. (3), Equation (3) can be rewritten as

$$\ln Z = \ln A + n\ln[\sinh(\alpha\sigma)]\,. \tag{4}$$

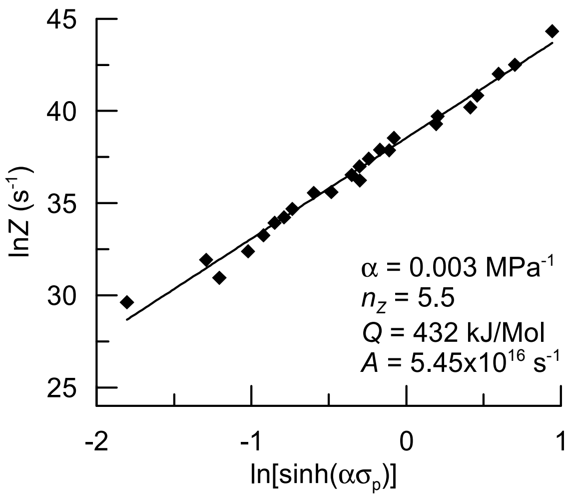

Fig. 7. Calculation of the Zener–Hollomon parameter of the hot deformed Hastelloy X superalloy.

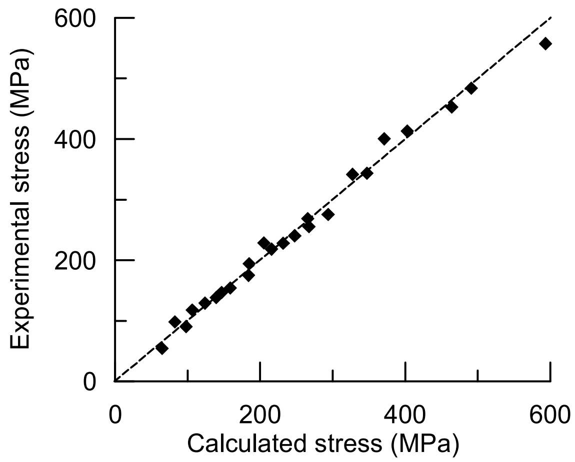

Fig. 8. Comparison between measured and calculated peak stresses. The dashed line indicates a perfect match between the calculation and measurement.

Equation (4) indicates that a linear relation should exist between ln[sinh($\alpha\sigma$)] and ln$Z$. The relationship between ln$Z$ and ln[sinh($\alpha\sigma_p$)] is given in Fig. 7. The linear relation between ln$Z$ and ln[sinh($\alpha\sigma_p$)] indicates that the relation of the peak stress with the strain rate and temperature satisfies Eq. (4) well for Hastelloy X superalloy. The coefficient of determination R^2 of the fit is 0.99. By substituting the calculated parameters into Eq. (1), the constitutive equation can be obtained as

$$\dot{\varepsilon} = 5.45\times10^{16}[\sinh(0.003\sigma_p)]^{5.5}\exp\left[\frac{-432000}{RT}\right]. \quad (5)$$

The flow stresses calculated using Eq. (5) were compared with the measured flow stresses, as shown in Fig. 8. It is clear that the calculated stresses match the measured stresses well. The constitutive equation obtained in this work gives reasonable fit to the measured values.

Summary

The hot deformation behavior of a Hastelloy X Ni-base superalloy was investigated in compression at 900−1150 °C, with strain rates from 0.001 to 1 s^{-1}. The peak stress did not significantly decrease with increasing temperature at low strain rates. In contrast, the differences in the peak stress between different temperatures were much greater at high strain rates. Constitutive analysis indicated that the hot deformation behavior of the Hastelloy X superalloy satisfied the hyperbolic sine constitutive equation. The stress exponent n was 5.5. This result indicated that dislocation creep could be a dominant deformation process during hot deformation.

References

[1] S. Guo, D. Li, H. Pen, Q. Guo, J. Hu: J. Nuclear Mater. Vol. 410 (2011), p. 52
[2] S.L. Semiatin, P.N. Fagin, M.G. Glavicic, D. Raabe: Scripta Mater. Vol. 50 (2004), p. 625
[3] H.J. McQueen, C.A.C. Imbert: J. Alloys Compd. Vol. 378 (2004), p. 35
[4] Y.L. Fang, Z.Y. Liu, H.M. Song, L.Z. Jiang: Mater. Sci. Eng. A Vol. A526 (2009), p. 128
[5] C. Sellars, W.M. Tegart: Acta Metall. Vol. 14 (1966), p. 1136
[6] C. Sellars, W.M. Tegart: Int. Metall. Rev. Vol. 17 (1972), p. 1
[7] S.E. Hsu, G.R. Edwards, O.D. Sherby: Acta. Metall. Vol. 31 (1983), p. 763
[8] C. Zener, J.H. Hollomon: J. Appl. Phys. Vol. 15 (1944), p. 22

國科會補助計畫衍生研發成果推廣資料表

日期:2013/09/20

國科會補助計畫	計畫名稱: 鎳基超合金熱變形行為分析及組合關係探討
	計畫主持人: 吳泓瑜
	計畫編號: 101-2221-E-216-007- 學門領域: 航太科技

無研發成果推廣資料

101 年度專題研究計畫研究成果彙整表

計畫主持人：吳泓瑜	計畫編號：101-2221-E-216-007-
計畫名稱：鎳基超合金熱變形行為分析及組合關係探討	

成果項目			量化			單位	備註（質化說明：如數個計畫共同成果、成果列為該期刊之封面故事...等）
			實際已達成數（被接受或已發表）	預期總達成數(含實際已達成數)	本計畫實際貢獻百分比		
國內	論文著作	期刊論文	0	0	100%	篇	
		研究報告/技術報告	0	0	100%		
		研討會論文	1	1	100%		
		專書	0	0	100%		
	專利	申請中件數	0	0	100%	件	
		已獲得件數	0	0	100%		
	技術移轉	件數	0	0	100%	件	
		權利金	0	0	100%	千元	
	參與計畫人力（本國籍）	碩士生	2	2	100%	人次	
		博士生	0	0	100%		
		博士後研究員	0	0	100%		
		專任助理	0	0	100%		
國外	論文著作	期刊論文	0	1	100%	篇	
		研究報告/技術報告	1	1	100%		
		研討會論文	1	1	100%		
		專書	0	0	100%	章/本	
	專利	申請中件數	0	0	100%	件	
		已獲得件數	0	0	100%		
	技術移轉	件數	0	0	100%	件	
		權利金	0	0	100%	千元	
	參與計畫人力（外國籍）	碩士生	2	2	100%	人次	
		博士生	0	0	100%		
		博士後研究員	0	0	100%		
		專任助理	0	0	100%		

其他成果 (無法以量化表達之成果如辦理學術活動、獲得獎項、重要國際合作、研究成果國際影響力及其他協助產業技術發展之具體效益事項等，請以文字敘述填列。)	無

	成果項目	量化	名稱或內容性質簡述
科教處計畫加填項目	測驗工具(含質性與量性)	0	
	課程/模組	0	
	電腦及網路系統或工具	0	
	教材	0	
	舉辦之活動/競賽	0	
	研討會/工作坊	0	
	電子報、網站	0	
	計畫成果推廣之參與（閱聽）人數	0	

國科會補助專題研究計畫成果報告自評表

請就研究內容與原計畫相符程度、達成預期目標情況、研究成果之學術或應用價值（簡要敘述成果所代表之意義、價值、影響或進一步發展之可能性）、是否適合在學術期刊發表或申請專利、主要發現或其他有關價值等，作一綜合評估。

1. 請就研究內容與原計畫相符程度、達成預期目標情況作一綜合評估

■達成目標

□未達成目標（請說明，以 100 字為限）

□實驗失敗

□因故實驗中斷

□其他原因

說明：

2. 研究成果在學術期刊發表或申請專利等情形：

論文：■已發表 □未發表之文稿 □撰寫中 □無

專利：□已獲得 □申請中 ■無

技轉：□已技轉 □洽談中 ■無

其他：（以 100 字為限）

3. 請依學術成就、技術創新、社會影響等方面，評估研究成果之學術或應用價值（簡要敘述成果所代表之意義、價值、影響或進一步發展之可能性）（以 500 字為限）

本計畫主要探討 Hastelloy X 鎳基超合金的高溫流變性質及組合方程式的建立。以熱壓實驗所得之應力-應變關係獲得其組合方程式。本計畫對於高溫組合方程式中組合參數之計算提出新的分析模式，並與多數學者使用的方析方法比較，本計畫的成果可以對流變應力的模擬提供較精確的計算值。有關 Hastelloy X 鎳基超合金含應變影響之組合關係式，目前國內外均未見到相關學術論文發表。本研究計畫的成果，已發表國際學術研討會論文，論文收錄於 Applied Mechanics and Materials Vol. 252 (2013)EI 期刊論文中。期刊論文以 A flow stress modeling in annealed Hastelloy X superalloy under hot compression 為論文題目，已投寄國外 SCI 等級學術期刊。

2010 年 6 月國內相關產業成立了「台灣精製產業研發聯盟」，高溫合金關鍵零件製作技術的開發為主要項目之一。本計畫的執行，對國內高溫合金熱變形分析能力的建立具有前瞻性。本計畫的執行成果有助於建立國內自主開發材料之零件熱加工成形技術。高溫合金熱變形組合關係式主要用於熱加工過程流變應力的計算，未來結合國內超合金熔煉廠家；例如榮剛公司…等，配合本計畫所建立的熱加工性分析技術，可以達到國內航空、能源及精密製造產業等關鍵產品開發的目標。